Review Article
miR-140 promotes proliferation and cartilage differentiation of bone mesenchymal stem cells through inhibition of FGF9

Shaolin Ji[1], Yuezhen Ma[2], Lingling Jiang[2], Xiaodan Zhao[3]

Departments of [1]Trauma and Hand-foot Surgery, [2]Nursing, Shandong Provincial Third Hospital, Jinan 250000, Shandong, China; [3]Department of Intensive-care, Shandong Provincial Third Hospital, No. 12 Middle Wuying Mountain Road, Tianqiao District, Jinan 250000, Shandong, China

Abstract: Objective: This paper aimed to investigate miR-140 in promoting bone mesenchymal stem cells (BMSCs) to proliferate via targeting FGF9. Methods: Sixty-six bone marrow specimens from patients with osteoarthritis in the orthopedics department of our hospital from January 2018 to October 2019 were collected. A further 66 bone marrow specimens from healthy people during the same period were selected as controls. qPCR was adopted for detecting miR-140 expression in the two groups of bone marrow specimens. miR-140 overexpression vectors were constructed and then transfected into the BMSCs, whose proliferation, invasion, migration, and apoptosis were observed. Western blot was adopted for detecting cartilage differentiation markers (Sox9 and Has2). The binding site of miR-140 and FGF9 was predicted, and their targeted relationship was detected. Results: miR-140 expression downregulated in osteoarthritis (P<0.05), and its overexpression inhibited BMSCs to proliferate and promoted their apoptosis (P<0.05). Sox9 and Has2 were inhibited (P<0.05). According to dual luciferase reporter gene assay, luciferase activity remarkably reduced when miR-140 bound to FGF9 (P<0.05). Conclusion: miR-140 promotes the proliferation and cartilage differentiation of BMSCs via inhibiting FGF9.

Keywords: miR-140, FGF9, BMSCs, proliferation, cartilage differentiation

Introduction

Osteoarthritis is the main cause of joint pain and disability [1], characterized by arthralgia, tenderness, and constrained motion [2]. Affecting more than 25% of the population older than 18 years old, the disease may lead to pathological changes such as the gradual loss and destruction of articular cartilage [3]. In addition to causing disability, it affects people's physical health, and may negatively affect their mental health [4]. At present, the treatment of this disease lacks intervention measures that can change its natural course [5]. miRNAs are non-coding RNA molecules that act as negative regulators of gene expression and regulate a series of biological functions [6], exerting a pivotal function in cellular signal transduction and in vivo regulations [7]. miR-140, as one of them, is abnormally expressed in various diseases [8]. In an in vitro

model of human lung A549 cells, miR-140-5p downregulation increases levels of inflammatory cytokines induced by acute lung injury [9]. This miRNA is involved in nephroblastoma progression via targeting TGFBRI/SMAD2/3 and IGF-1R/AKT signaling pathways [10]. Additionally, low miR-140 expression is negatively correlated with the severity of osteoarthritis [11]. As a transcription factor related to gliogenesis in vertebrate central nervous system, Sox9 has strong gliogenesis activity [12]. Sox9 and hyaluronic acid synthase 2 (Has2) are both chondrogenesis markers [13]. Fibroblast growth factor 9 (FGF9) belongs to the fibroblast growth factor family and is involved in a series of biological processes including tumor growth and invasion [14]. During skeletal development, this factor has a complex and important effect on endochondral ossification and intramembranous bone formation [15]. miR-140 is an effective chondrogenic differen-

Table 1. Primer sequences

	Upstream primers (5'-3')	Downstream primers (5'-3')
miR-140	GCGGCGGCAGTGGTTTTACCC	ATCCAGTGCAGGGTCCGAGG
U6	CTCGCTTCGGCAGCACA	AACGCTTCACGAATTTGCGT

tiation inducer of human bone mesenchymal stem cells (BMSCs) [16], and miR-140-5p inhibits tumor growth and metastasis by inhibiting FGF9 expression in hepatocellular carcinoma [17]. This suggests that miR-140 and FGF9 have an influence on the biological mechanism of cells. Therefore, effects of miR-140 on BMSCs through targeting FGF9 were explored in this study.

Materials and methods

Specimen collection

Sixty-six bone marrow specimens from patients with osteoarthritis in the orthopedics department of our hospital from January 2018 to October 2019 were collected, consisting of 38 males and 28 females. Another 66 bone marrow specimens from healthy people during the same period were selected as controls, consisting of 35 males and 31 females.

Inclusion and exclusion criteria

Inclusion criteria: Those who were diagnosed with osteoarthritis by rheumatoid factor test [18] and had complete clinical data. The study was approved by the Ethics Committee of Shandong Provincial Third Hospital. Patients and their family members were informed in advance of this experiment and signed the informed consent form.

Exclusion criteria: Those with severe hepatic and renal insufficiency; those who had received other treatments before.

Main instruments and materials

Human BMSCs were purchased from Shanghai Huzhen Industrial Co., Ltd. Real-time fluorescence quantitative PCR instrument was purchased from Guangzhou Huafeng Biological Technology Co., Ltd. Apoptosis detection kit was purchased from Hangzhou Bever Medical Devices Co. Ltd. Trizol reagent was purchased from Beijing Biolab Science And Technology Co., Ltd. 10% fetal bovine serum (FBS) was purchased from Shanghai Lianshuobao is

Biotechnology Co., Ltd. DMEM was purchased from Jieshikang Biotechnology Co., Ltd., Qingdao. Transfection reagent Lipofectamine TM2000 was purchased from Suzhou Yuheng Biological Technology Co., Ltd. CCK8 assay kit was purchased from G-CLONE, Beijing. Ultraviolet spectrophotometer was purchased from Clinx Science Instruments, Shanghai. BD flow cytometer was purchased from Derica Biotech, Beijing. Transwell chamber was purchased from Shanghai SunBio Biomedical Technology Co., Ltd. Reverse transcriptase was purchased from Shanghai Kang Lang Biological Technology Co., Ltd. Microplate reader was purchased from Beijing Image Trading Co., Ltd. Paraformaldehyde was purchased from Zibo Qixing Chemical Technology Co., Ltd. Crystal violet stain was purchased from Shenzhen Xinyaosheng Industrial Co., Ltd. Primers for miR-140 and internal reference were synthesized by Beijing Sino-US Taihe Biotechnology Co., Ltd. See **Table 1** for details.

Methods

Detection of miR-140 expression by qPCR: miR-140 expression in bone marrow specimens from patients with osteoarthritis and healthy people was detected by qRT-PCR, and total RNA was extracted from the specimens using the Trizol reagent, with the steps strictly performed based on the kit instructions. The concentration and purity of the total RNA were detected by the UV spectrophotometer. The RNA with OD260/OD280 between 1.8-2.0 was taken out for cDNA synthesis using reverse transcriptase and oligonucleotide according to the kit instructions. Transcription reaction system (total 20 μL) was composed of buffer (4 μL), reverse transcriptase (2 μL), total RNA (2 μL), and RNase-free water (12 μL). The reaction conditions were water bath at 42°C for 1 hour and then at 95°C for 5 minutes. Amplification was performed on the PCR instrument, with GADPH as an internal reference control. miR-140 expression was detected on the fluorescence quantitative PCR instrument using miR-140 specific primers based on the kit instructions. PCR system (total 20 μL) was composed of upstream primer (0.4 μL), downstream primer (0.4 μL), Taq DNA Polymerase (0.5 μL), and ddH$_2$O added to make up to the system. The reaction condition

was 94°C for 10 s, and then cycling (94°C for 5 s, annealing at 52°C for 30 s, 72°C for 15 s) for 40 times. Three replicate wells were provided for each experiment. Three repeated experiments were carried out. The experimental results were analyzed by relative quantification, and relative miR-140 expression was calculated by 2-ΔΔCT.

Cell culture and transfection: The cells were conventionally sub-cultured in a high-glucose DMEM (10% FBS solution +1% penicillin/streptomycin solution) in an incubator (37°C, 5% CO_2). They were inoculated into a 6-well plate to allow their density reach 60%-70%. miR-140-mimics and NC-mimics were transfected into the cells with the Lipofectamine TM2000 kit based on the instruction.

Detection of cell growth curve: The transfected BMSCs were prepared into a cell suspension, which was inoculated into a 96-well plate at 100 μL/well, with each well provided with 3 same wells. Each well was mixed with 20 μL of cell proliferation colorimetric assay reagent (CCK-8) at 24, 48, 72, and 96 hours, respectively, and then cultured in the incubator (37°C, 5% CO_2) for 2 hours. Next, the optical density (OD) value at 490 nm was measured by a fully automated microplate reader, so as to observe cell proliferation. Three repeated experiments were conducted.

Detection of cell migration and invasion: The cells were first digested with trypsin, and then resuspended with serum-free medium. The resuspension (200 μL) was used for migration determination, and approximately $5×10^4$ cells were placed in the upper chamber of the Transwell. Another resuspension (200 μL) was taken for invasion determination, and approximately $5×10^4$ cells together with FBS-containing medium (1 mL) were added to the lower chamber of the 6-well plate. After 24-hour conventional culture, the cells in the upper chamber were wiped off with cotton swabs, while those migrating to the lower chamber were fixed with 4% paraformaldehyde and stained with 0.1% crystal violet. After the Transwell chamber was dried, a membrane was prepared and sealed. The number of cells penetrating the membrane was observed and counted under an optical microscope. Three repeated experiments were conducted.

Detection of cell apoptosis: The apoptosis assay kit was used to detect cell apoptosis according to the kit's instruction. The BD flow cytometer was used to detect the cells transfected for 48 hours and stained with Annexin V and PI in the 6-well plate. Three repeated experiments were conducted.

Detection of Sox9 and Has2 expression by Western blot (WB): RIPA buffer was used to lyse total cell protein. The same amount of protein was separated by 10% SDS-PACE, transferred to PVDF membrane, and then sealed for 1 hour. After addition with universal secondary antibody (goat anti-rabbit, Shanghai YuanMu Biological Technology Co., Ltd.), the membrane reacted at room temperature for 2 hours, was then cleaned 3 times, and then fixed and developed in the ECL color development system.

Detection of targeted relationship between miR-140 and FGF9 by dual luciferase reporter gene assay (DLRGA): The DNA fragment of FGF9mRNA 3'-UTR containing the miR-140 putative binding site was synthesized. Next, the fragment was sub-cloned to the Xho I and Not I sites downstream of the renilla luciferase coding region of psiCHECK-2 vector, which was verified by Sangon Biotech sequencing. PsiCHECK2-FGF9-wt or PsiCHECK2-FGF9-mut was constructed, and then miR-140-mimics or miR-NC and Wt-FGF9 or Mut-FGF9 were transfected into the BMSCs using the Lipofectamine TM2000. The cells were collected after 48-hour transfection. Firefly and renilla luciferase activities were analyzed using DLRGA (Promega) based on the manufacturer's instruction.

Statistical analysis

The differences were verified by SPSS 20.0 (SPSS, Inc., Chicago, IL, USA). Measurement data were analyzed by t test, expressed by mean ± standard deviation ($\overline{x}$ ± sd). The comparison between multiple time points within groups was analyzed by repeated measures analysis of variance, and represented by F. The difference was statistically significant when $P<0.05$.

Results

Relative miR-140 expression

Relative miR-140 expression was (0.86±0.15) in the bone marrow specimens from patients with osteoarthritis and (2.26±0.04) in those
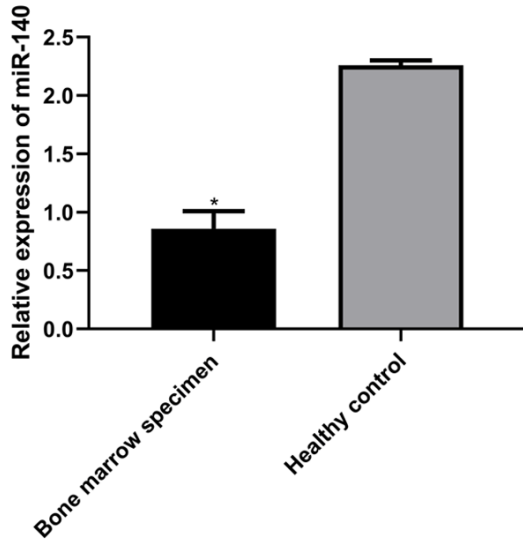
Figure 1. Relative miR-140 expression. Relative miR-140 expression was lower in the bone marrow specimens from patients with osteoarthritis (P<0.05). Note: * indicates the comparison with healthy people (P<0.05).
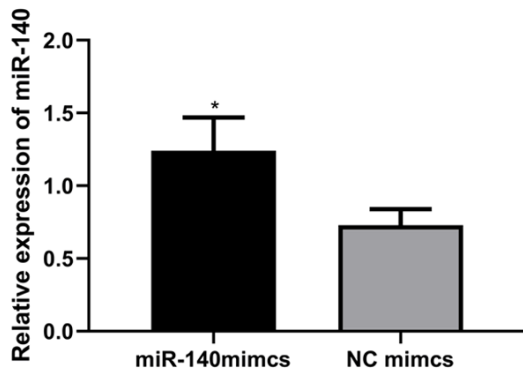

Figure 2. Effects of miR-140 after transfection with mimics. After transfection, relative miR-140 expression was remarkably higher in the miR-140-mimics group (P<0.05). Note: * indicates the comparison with the NC-mimics group (P<0.05).

from healthy people. The relative expression was lower in those from the patients with osteoarthritis (P<0.05). See **Figure 1** for details.

Effects of miR-140 after transfection with mimics

After transfection, miR-140 expression was (1.24±0.23) in the miR-140-mimics group and (0.73±0.11) in the NC-mimics group. After transfection, the expression was higher in the miR-140-mimics group (P<0.05), indicating
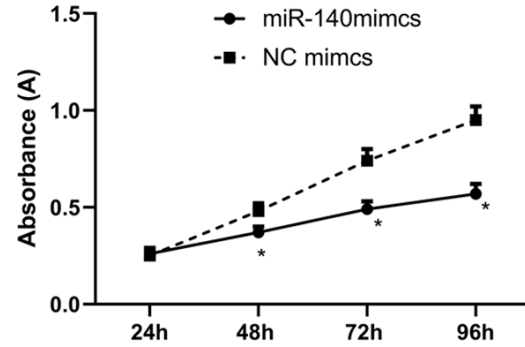

Figure 3. Growth of BMSCs at different time periods after transfection. From 0 h to 24 h, the difference was not significant in BMSC growth between the miR-140-mimics and NC-mimics groups (P>0.05), while from 48 h to 96 h, the growth was remarkably lower in the miR-140-mimics group (P<0.05). Note: * indicates the comparison with the NC-mimics group (P<0.05).

that miR-140 has a clear upregulation effect (P<0.05). See **Figure 2** for details.

Growth of BMSCs at different time periods after transfection

From 0 h to 24 h, the difference was not significant in BMSC growth between the miR-140-mimics and NC-mimics groups (P>0.05), while from 48 h to 96 h, the growth was lower in the miR-140-mimics group (P<0.05). See **Figure 3** for details.

BMSC migration and invasion after transfection

After transfection, the migration number of BMSCs was (83.28±8.47) in the miR-140-mimics group and (165.29±15.34) in the NC-mimics group. The migration number was lower in the miR-140-mimics group (P<0.05). See **Figure 4** for details. After transfection, the invasion number of BMSCs was (74.12±7.22) in the miR-140-mimics group and (153.15±14.29) in the NC-mimics group. The invasion number was lower in the miR-140-mimics group (P<0.05). See **Figure 5** for details.

Apoptotic rate of BMSCs after transfection

After transfection, the apoptotic rate of BMSCs was (27.33±4.23)% in the miR-140-mimics group and (5.46±1.45)% in the NC-mimics group. The apoptotic rate was higher in the miR-
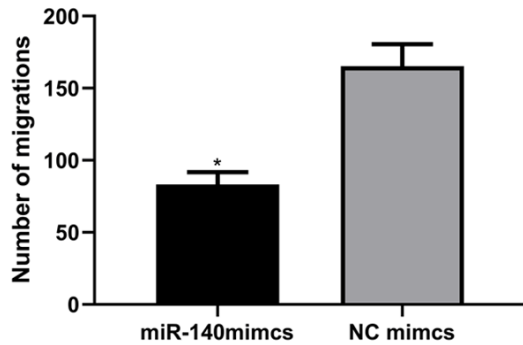
Figure 4. BMSC migration after transfection. After transfection, the migration number of BMSCs was remarkably lower in the miR-140-mimics group (P<0.05). Note: * indicates the comparison with the NC-mimics group (P<0.05).
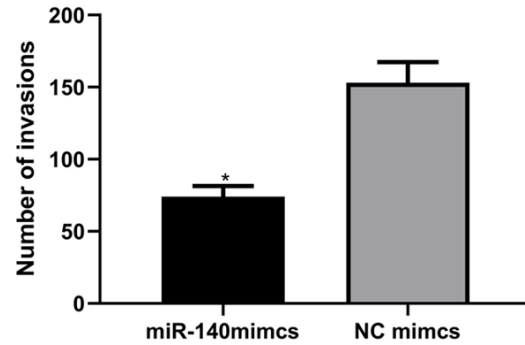

Figure 5. BMSC invasion after transfection. After transfection, the invasion number of BMSCs was remarkably lower in the miR-140-mimics group (P<0.05). Note: * indicates the comparison with the NC-mimics group (P<0.05).

140-mimics group (P<0.05). See **Figure 6** for details.

Sox9 and Has2 protein expression levels

Sox9 protein expression was (0.52±0.04) in the miR-140-mimics group and (1.13±0.23) in the NC-mimics group. Has2 protein expression was (0.45±0.02) in the miR-140-mimics group and (1.21±0.24) in the NC-mimics group. Sox9 and Has2 protein expression reduced in the miR-140-mimics group (P<0.05). See **Figure 7** for details.

miR-140 directly targeted FGF9

The binding site between miR-140 and FGF9 was predicted through Starbase. According to DLRGA, miR-140-mimics could reduce FGF9-Wt luciferase activity, but it did not affect FGF9-Mut luciferase activity. This indicates that miR-140 binding to FGF9 could remarkably reduce luciferase activity (P<0.05). See **Figure 8** for details. Next, we observed the effects of interfering with FGF9 on BMSCs, so FGF9 was re-expressed in the cells transfected with miR-140. The results showed that the re-expression rescued the migration and invasion and growth defects of miR-140 in the cells expressing this miRNA. See **Figure 9** for details.

Discussion

qPCR was adopted for detecting relative miR-140 expression in the bone marrow specimens from patients with osteoarthritis and healthy people. The relative expression was lower in those from the osteoarthritis patients,

which suggests that miR-140 expression is downregulated in osteoarthritis. According to similar studies, miR-140 expression is remarkably reduced in the synovial fluid of patients with the disease [19], and the expression in synovium may be an early diagnostic marker for knee osteoarthritis. Therefore, miR-140 expression can be used as an indicator of osteoarthritis progression [20]. In another study, Hsa-miR-140-3p expression in the articular cartilage of patients with osteoarthritis continuously reduced compared with healthy individuals [21]. These findings reveal that miR-140 can be used as a pathogenic detecting factor, and its continuous decrease may be related to the adverse development of the disease. Therefore, we observed the biological mechanisms of BMSCs by transfecting miR-140-mimics, and found that their proliferation was inhibited and their apoptosis was induced. Some studies have shown that miR-140-5p inhibits the IL-1β-induced inflammation of chondrocytes via regulating HMGB1 in osteoarthritis [22]. This miRNA is downregulated in synovial tissues and cells in knee osteoarthritis. In addition, its upregulation can inhibit inflammatory responses and the apoptosis of synovial cells, and promotes cell proliferation, thus protecting synovial injury in the knee of rats with osteoarthritis [23]. Moreover, miR-140 is also downregulated in gastric cancer cells, and miR-140-5p directly targets YES1 to inhibit the biological mechanism of the cells [24]. All of these factors demonstrate that osteoarthritis progression can be alleviated by regulating biological effects of miR-140 on BMSCs.
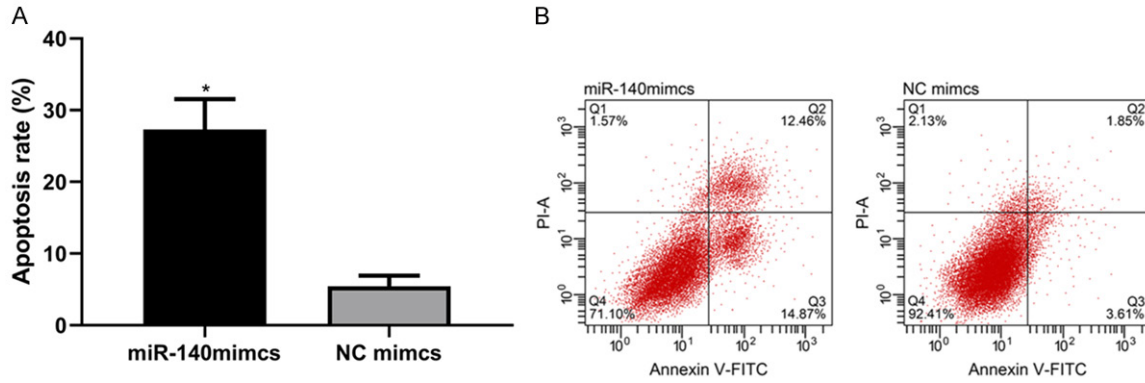
Figure 6. Apoptotic rate of BMSCs after transfection. A. After transfection, the apoptotic rate of BMSCs was remarkably higher in the miR-140-mimics group (P<0.05). Note: * indicates the comparison with the NC-mimics group (P<0.05). B. Flow cytometry maps.
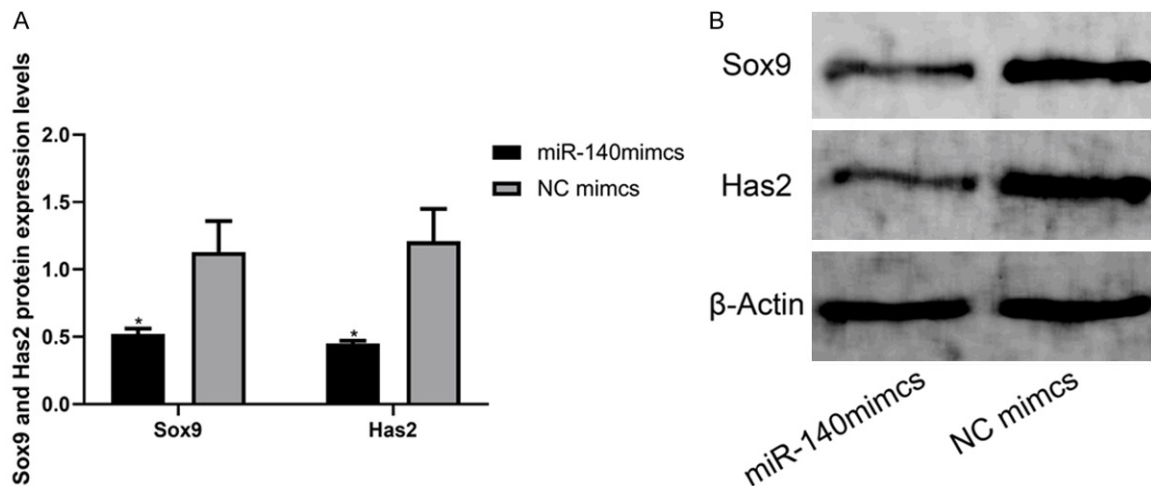

Figure 7. Sox9 and Has2 protein expression levels. A. Sox9 and Has2 protein expression remarkably reduced in the miR-140-mimics group (P<0.05). Note: * indicates the comparison with the NC-mimics group (P<0.05). B. A WB diagram.
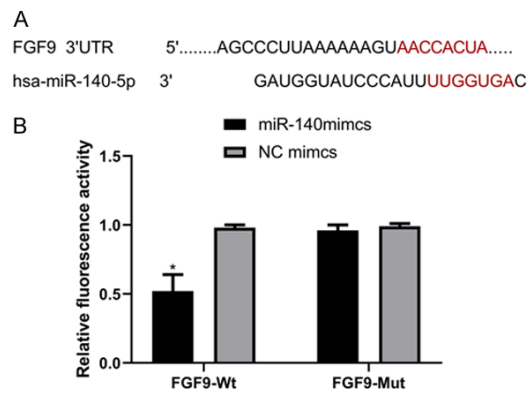

Figure 8. Results of DLRGA. A. miR-140 and FGF9 have a binding site. B. miR-140-mimics could reduce FGF9-Wt luciferase activity, but it did not affect FGF9-Mut luciferase activity. This indicates that miR-140 binding to FGF9 can remarkably reduce the luciferase activity (P<0.05). Note: * indicates the comparison with the NC-mimics group (P<0.05).

Sox9 is a crucial transcription factor in development and adult cartilage. Its genes are expressed in pluripotent bone progenitor cells and active during chondrocyte differentiation. It ensures chondrocytes following the promise, promotes cell survival, and transcribes and activates many cartilage specific structural components and genes of regulatory factors [25]. Hyaluronic acid aggrecan contributes to the cell spacing in cartilage. The former is synthesized by Has2 in cartilage, and its function is to anchor the latter on the sur-
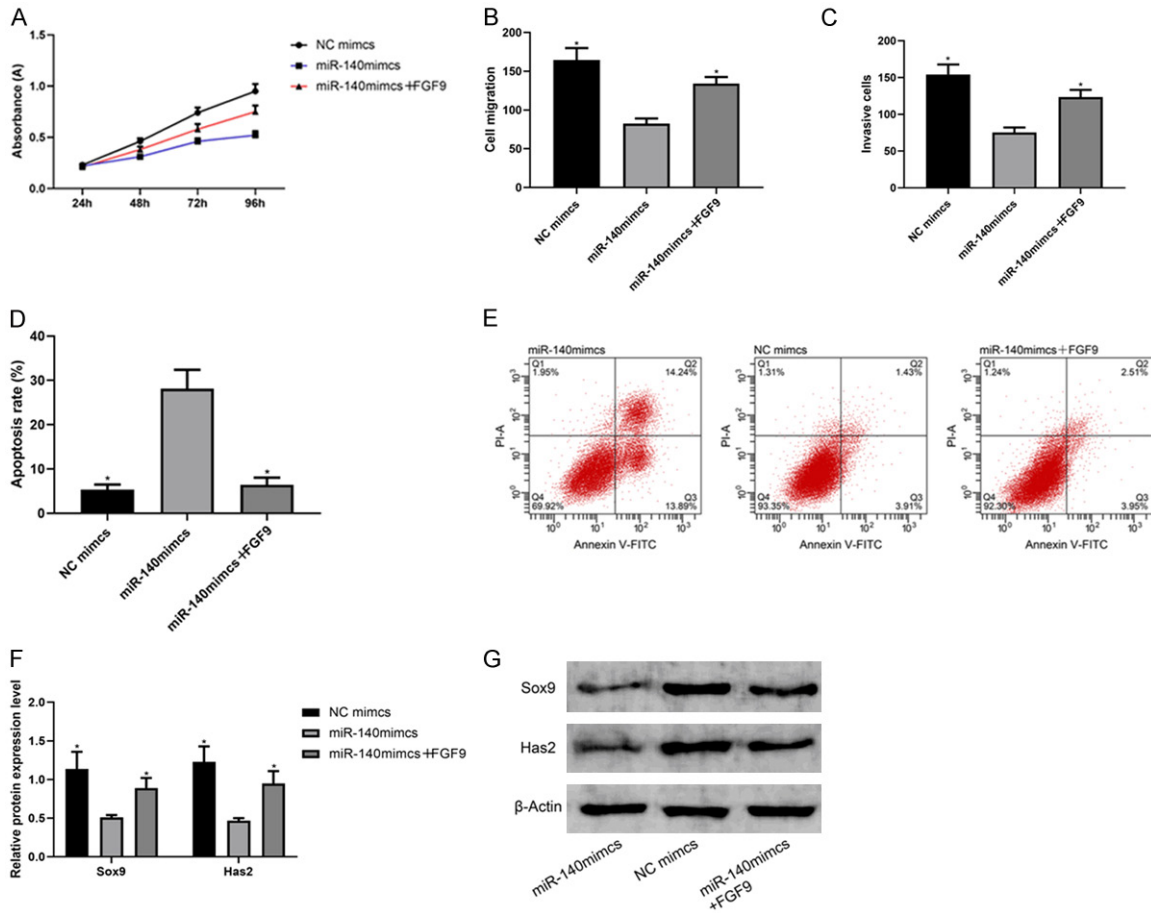
Figure 9. Effects of interfering with FGF9 on BMSCs. A. BMSC growth after interfering with FGF9. From 0 h to 24 h, the difference was not significant in BMSC growth between the NC-mimics, miR-140-mimics, and miR-140-mimics + FGF9 groups (P>0.05). From 48 h to 96 h, the growth in the miR-140-mimics group was lower than that in the NC-mimics group (P<0.05), while the growth in the miR-140-mimics + FGF9 group was remarkably higher than that in the miR-140-mimics group (P<0.05). Note: * indicates the comparison with the miR-140-mimics group (P<0.05). B. BMSC migration after interfering with FGF9. BMSC migration in the miR-140-mimics group was lower than that in the NC-mimics group (P<0.05), while the migration in the miR-140-mimics + FGF9 group was remarkably higher than that in the miR-140-mimics group (P<0.05). Note: * indicates the comparison with the miR-140-mimics group (P<0.05). C. BMSC invasion after interfering with FGF9. BMSC invasion in the miR-140-mimics group was lower than that in the NC-mimics group (P<0.05), while the invasion in the miR-140-mimics + FGF9 group was remarkably higher than that in the miR-140-mimics group (P<0.05). Note: * indicates the comparison with the miR-140-mimics group (P<0.05). D. BMSC apoptosis after interfering with FGF9. BMSC apoptosis in the miR-140-mimics group was higher than that in the NC-mimics group (P<0.05), while the apoptosis in the miR-140-mimics + FGF9 group was remarkably lower than that in the miR-140-mimics group (P<0.05). Note: * indicates the comparison with the miR-140-mimics group (P<0.05). E. Flow cytometry maps. F. Sox9 and Has2 protein expression levels after interference with FGF9. Sox9 and Has2 protein expression in the miR-140-mimics group was lower than that in the NC-mimics group (P<0.05), while the protein expression in the miR-140-mimics + FGF9 group was remarkably higher than that in the miR-140-mimics group (P<0.05). Note: * indicates the comparison with the miR-140-mimics group (P<0.05). G. A WB diagram.

face of chondrocytes [26]. Sox9 and Has2 have a great effect on chondrogenesis. In our study, miR-140 upregulation inhibited Sox9 and Has2 expression, indicating that the upregulation may alleviate cartilage differentiation. According to some studies, compared with normal human umbilical cord mesenchymal stem cells, the intra-articular injection of 140-MSC remarkably enhances the self-repair of articular cartilage [27]. miR-140 can relieve early osteoarthritis progression by delaying chondrocyte aging, thereby providing new evidence for the miR-mediated epigenetic regulation of chondrocyte aging to participate in disease

pathogenesis [28]. Moreover, the intra-articular injection of miR-140 can alleviate osteoarthritis progression through regulating the ECM steady state of rats, so it may be a new therapy for the disease [29], and may benefit patients with early osteoarthritis [30]. Finally, we found that miR-140 and FGF9 have a binding site, and that miR-140 binding to FGF9 reduced luciferase activity. This suggests that miR-140 may promote BMSC proliferation and cartilage differentiation via targeting FGF9. Although there has been no clear study to show that miR-140 targets FGF9 to inhibit BMSC proliferation, other similar studies have revealed that miR-140-5p inhibits laryngeal squamous cell carcinoma partially through regulating FGF9 expression [31].

In summary, miR-140 may alleviate BMSC proliferation and cartilage differentiation via interaction with FGF9.

Disclosure of conflict of interest

None.

Address correspondence to: Xiaodan Zhao, Department of Intensive-Care, Shandong Provincial Third Hospital, No. 12 Middle Wuying Mountain Road, Tianqiao District, Jinan 250000, Shandong, China. Tel: +86-18830906868; E-mail: zhaowbcx94460@163.com

References

[1] Mathiessen A and Conaghan PG. Synovitis in osteoarthritis: current understanding with therapeutic implications. Arthritis Res Ther 2017; 19: 18.

[2] Bartels EM, Juhl CB, Christensen R, Hagen KB, Danneskiold-Samsoe B, Dagfinrud H and Lund H. Aquatic exercise for the treatment of knee and hip osteoarthritis. Cochrane Database Syst Rev 2016; 3: CD005523.

[3] Chen D, Shen J, Zhao W, Wang T, Han L, Hamilton JL and Im HJ. Osteoarthritis: toward a comprehensive understanding of pathological mechanism. Bone Res 2017; 5: 16044.

[4] Vina ER and Kwoh CK. Epidemiology of osteoarthritis: literature update. Curr Opin Rheumatol 2018; 30: 160-167.

[5] Collins JA, Diekman BO and Loeser RF. Targeting aging for disease modification in osteoarthritis. Curr Opin Rheumatol 2018; 30: 101-107.

[6] Ganju A, Khan S, Hafeez BB, Behrman SW, Yallapu MM, Chauhan SC and Jaggi M. miRNA nanotherapeutics for cancer. Drug Discov Today 2017; 22: 424-432.

[7] Rupaimoole R, Calin GA, Lopez-Berestein G and Sood AK. miRNA deregulation in cancer cells and the tumor microenvironment. Cancer Discov 2016; 6: 235-246.

[8] Fang Z, Yin S, Sun R, Zhang S, Fu M, Wu Y, Zhang T, Khaliq J and Li Y. miR-140-5p suppresses the proliferation, migration and invasion of gastric cancer by regulating YES1. Mol Cancer 2017; 16: 139.

[9] Yang Y, Liu D, Xi Y, Li J, Liu B and Li J. Upregulation of miRNA-140-5p inhibits inflammatory cytokines in acute lung injury through the MyD88/NF-kappaB signaling pathway by targeting TLR4. Exp Ther Med 2018; 16: 3913-3920.

[10] Liu Z, He F, OuYang S, Li Y, Ma F, Chang H, Cao D and Wu J. miR-140-5p could suppress tumor proliferation and progression by targeting TGF-BRI/SMAD2/3 and IGF-1R/AKT signaling pathways in Wilms' tumor. BMC Cancer 2019; 19: 405.

[11] Si H, Zeng Y, Zhou Z, Pei F, Lu Y, Cheng J and Shen B. Expression of miRNA-140 in chondrocytes and synovial fluid of knee joints in patients with osteoarthritis. Chin Med Sci J 2016; 31: 207-212.

[12] Vogel JK, Weider M, Engler LA, Hillgartner S, Schmitt C, Hermans-Borgmeyer I and Wegner M. Sox9 overexpression exerts multiple stage-dependent effects on mouse spinal cord development. Glia 2020; 68: 932-946.

[13] Zhang Y, Huang X and Yuan Y. MicroRNA-410 promotes chondrogenic differentiation of human bone marrow mesenchymal stem cells through down-regulating Wnt3a. Am J Transl Res 2017; 9: 136-145.

[14] Wang Q, Liu S, Zhao X, Wang Y, Tian D and Jiang W. MiR-372-3p promotes cell growth and metastasis by targeting FGF9 in lung squamous cell carcinoma. Cancer Med 2017; 6: 1323-1330.

[15] Lu J, Dai J, Wang X, Zhang M, Zhang P, Sun H, Zhang X, Yu H, Zhang W, Zhang L, Jiang X and Shen SG. Effect of fibroblast growth factor 9 on the osteogenic differentiation of bone marrow stromal stem cells and dental pulp stem cells. Mol Med Rep 2015; 11: 1661-1668.

[16] Mahboudi H, Soleimani M, Hanaee-Ahvaz H, Ghanbarian H, Bandehpour M, Enderami SE and Kazemi B. New approach for differentiation of bone marrow mesenchymal stem cells toward chondrocyte cells with overexpression of microRNA-140. ASAIO J 2018; 64: 662-672.

[17] Wang W, Dong Y, Li X, Pan Y, Du J and Liu D. MicroRNA-431 serves as a tumor inhibitor in breast cancer through targeting FGF9. Oncol Lett 2020; 19: 1001-1007.

[18] Hinton R, Moody RL, Davis AW and Thomas SF. Osteoarthritis: diagnosis and therapeutic considerations. Am Fam Physician 2002; 65: 841-848.

[19] Yang R, Zhang D, Yu K, Sun L, Yang J, Zhao C, Li X and Chen Y. Detection of miR-22, miR-140 and bone morphogenetic proteins (BMP)-2 expression levels in synovial fluid of osteoarthritis patients before and after arthroscopic debridement. Med Sci Monit 2018; 24: 863-868.

[20] Chao Y, Zhang L, Zhang X, Ma C and Chen Z. Expression of MiR-140 and MiR-199 in synovia and its correlation with the progression of knee osteoarthritis. Med Sci Monit 2020; 26: e918174.

[21] Ntoumou E, Tzetis M, Braoudaki M, Lambrou G, Poulou M, Malizos K, Stefanou N, Anastasopoulou L and Tsezou A. Serum microRNA array analysis identifies miR-140-3p, miR-33b-3p and miR-671-3p as potential osteoarthritis biomarkers involved in metabolic processes. Clin Epigenetics 2017; 9: 127.

[22] Wang Y, Shen S, Li Z, Li W and Weng X. MIR-140-5p affects chondrocyte proliferation, apoptosis, and inflammation by targeting HMGB1 in osteoarthritis. Inflamm Res 2020; 69: 63-73.

[23] Huang X, Qiao F and Xue P. The protective role of microRNA-140-5p in synovial injury of rats with knee osteoarthritis via inactivating the TLR4/Myd88/NF-kappaB signaling pathway. Cell Cycle 2019; 18: 2344-2358.

[24] Fang Z, Yin S, Sun R, Zhang S, Fu M, Wu Y, Zhang T, Khaliq J and Li Y. miR-140-5p suppresses the proliferation, migration and invasion of gastric cancer by regulating YES1. Mol Cancer 2017; 16: 139.

[25] Lefebvre V and Dvir-Ginzberg M. SOX9 and the many facets of its regulation in the chondrocyte lineage. Connect Tissue Res 2017; 58: 2-14.

[26] Knudson W, Ishizuka S, Terabe K, Askew EB and Knudson CB. The pericellular hyaluronan of articular chondrocytes. Matrix Biol 2019; 78-79: 32-46.

[27] Geng Y, Chen J, Alahdal M, Chang C, Duan L, Zhu W, Mou L, Xiong J, Wang M and Wang D. Intra-articular injection of hUC-MSCs expressing miR-140-5p induces cartilage self-repairing in the rat osteoarthritis. J Bone Miner Metab 2019;

[28] Si HB, Yang TM, Li L, Tian M, Zhou L, Li DP, Huang Q, Kang PD, Yang J, Zhou ZK, Cheng JQ and Shen B. miR-140 attenuates the progression of early-stage osteoarthritis by retarding chondrocyte senescence. Mol Ther Nucleic Acids 2019; 19: 15-30.

[29] Si HB, Zeng Y, Liu SY, Zhou ZK, Chen YN, Cheng JQ, Lu YR and Shen B. Intra-articular injection of microRNA-140 (miRNA-140) alleviates osteoarthritis (OA) progression by modulating extracellular matrix (ECM) homeostasis in rats. Osteoarthritis Cartilage 2017; 25: 1698-1707.

[30] Karlsen TA, de Souza GA, Odegaard B, Engebretsen L and Brinchmann JE. microRNA-140 inhibits inflammation and stimulates chondrogenesis in a model of interleukin 1beta-induced osteoarthritis. Mol Ther Nucleic Acids 2016; 5: e373.

[31] Wang Y, Huang Q and Li F. miR-140-5p targeted FGF9 and inhibited the cell growth of laryngeal squamous cell carcinoma. Biochem Cell Biol 2020; 98: 83-89.